Algorithms for calculation of sunlight fluxes in the cloudy and cloudless atmosphere

T.B. Zhuravleva and K.M. Firsov

Institute of Atmospheric Optics, Siberian Branch of the Russian Academy of Sciences, Tomsk

Received September 8, 2004

This paper describes the statistical algorithms for calculation of solar spectral fluxes in the atmosphere under clear-sky and overcast conditions, as well as for the case of broken clouds. These algorithms are based on the representation of the transmission function of atmospheric gases in the form of an exponential series (k-distribution method). Molecular absorption coefficients are calculated using the HITRAN-2000 database with the allowance made for instrumental functions of the measurement facilities used, real meteorological parameters of the atmosphere, and gas concentration profiles. To test these algorithms, we compare our results with the reference data of line-by-line calculations of the up and downwelling fluxes for the clear sky and to the data of field measurements under overcast conditions. It is shown that the algorithms proposed are highly accurate and easy in computer realization.

Introduction

The most radiative experiments involve measurements of spectrally integral fluxes of solar radiation. At the same time, for better understanding of the mechanisms of sunlight interaction with the cloud, aerosol, and gas components of the atmosphere, it is necessary to have the information on the *spectral* distribution of radiative characteristics. Comparing experimental data with the results calculated for narrow spectral ranges, one could assess the capabilities of different radiation codes to adequately simulate the processes of sunlight transfer in the atmosphere–surface system. These codes differ by the methods of taking into account the molecular absorption and by the methods of solution of the radiative transfer equation.

For the last decade, Atmospheric and Environmental Research, Inc. (AER) (USA) have developed a number of well known models for calculation of monochromatic and broadband radiative fluxes in the spectral regions from the UV to microwaves. These models are based on the line-by-line Radiative Transfer Model (LBLRTM).[1] The LBLRTM capabilities were extended in the Code for High Resolution Accelerated Radiative Transfer (CHARTS) by taking into account the interaction of the optical radiation with clouds and aerosol on the assumption of the *horizontally homogeneous* atmosphere.[2]

An algorithm for calculation of spectral sunlight fluxes by the Monte Carlo method, which allows for the 3D effects of clouds, was proposed in Ref. 3. The latest modification of this model[4] permits the calculation of the spectral fluxes and warming/cooling rates based on the k-distribution method for 550 bands in the 0.2–5.0 μm range.

An effective method for calculation of *average* (over the set of realizations of cloud fields) spectral sunlight fluxes in the visible and near IR regions is reported in Ref. 5. This algorithm is based on the Monte Carlo method applied to solution of the system of closed equations for the average intensity in the statistically homogeneous Poisson model of broken clouds. In Ref. 5, the capabilities of this method were demonstrated by using the transmission functions of atmospheric gases proposed in Refs. 6 and 7. These parameterizations were developed in the late 1960s–early 1970s for the main absorption bands of atmospheric gases (H_2O, CO_2, O_3, CH_4, N_2O, N_2) and corresponded to the spectral resolution $\Delta\nu$ = 10–20 cm^{-1}. The spectroscopic information accumulated by now allows us to obtain more accurate parameterizations of the transmission functions and, consequently, to describe the atmospheric transfer of the optical radiation more adequately.

The aim of this work was to improve the algorithm proposed in Ref. 5 for the calculation of the average radiative characteristics of solar radiation in broken clouds with the aid of representation of the transmission function of atmospheric gases in the form of the exponential series (k-distribution method). The molecular absorption coefficients were calculated based on the HITRAN-2000 database taking into account the instrumental functions of the devices employed and real meteorological parameters of the atmosphere as well as the gas concentration profiles. In addition, this paper presents the algorithms developed for calculation of spectral sunlight fluxes under clear sky conditions and the conditions of continuous, horizontally homogeneous cloudiness.

1. The *k*-distribution method

To take into account the molecular absorption, we used the modified method of exponential series.[8] The transmission function caused by the molecular

0235-6880/04/11 799-08 $02.00

absorption of solar radiation in the spectral range $\Delta\lambda = (\lambda_1, \lambda_2)$ can be represented in the form:

$$T_{\Delta\lambda}(m) = \int_{\lambda_1}^{\lambda_2} F^*(\lambda) I_0(\lambda) T(m,\lambda)\mathrm{d}\lambda \Big/ I_{0,\Delta\lambda},$$

$$I_{0,\Delta\lambda} = \int_{\lambda_1}^{\lambda_2} F^*(\lambda) I_0(\lambda)\mathrm{d}\lambda, \quad (1)$$

where $F^*(\lambda)$ is the instrumental function of the detector; $I_0(\lambda)$ is the spectral solar constant;

$$T(m,\lambda) = \exp\left(-m \int_0^{H_{\mathrm{atm}}} \kappa_{\mathrm{mol}}(\lambda, z)\mathrm{d}z\right)$$

is the monochromatic transmission function of the Earth's atmosphere, $\kappa_{\mathrm{mol}}(\lambda, z)$ is the molecular absorption coefficient at the wavelength λ and the altitude z above the Earth's surface, m is the optical mass of the atmosphere (along the direction toward the Sun), H_{atm} is the top of the atmosphere. Assuming the Earth's atmosphere to be plane-parallel, $m = 1/\cos\xi_\odot$; $\xi_\odot$ is the solar zenith angle.

According to Ref. 8, $T_{\Delta\lambda}(m)$ can be transformed to the form

$$T_{\Delta\lambda}(m) = \int_0^1 \exp\left(-m \int_0^{H_{\mathrm{atm}}} k(g,z)\mathrm{d}z\right)\mathrm{d}g =$$

$$= \sum_{i=1}^{N} C_i \exp\left(-m \int_0^{H_{\mathrm{atm}}} k(g_i,z)\mathrm{d}z\right), \quad (2)$$

where $k(g, z)$ is the effective absorption coefficient in the space of cumulative frequencies, which is a continuous, increasing function of the argument g. The latter circumstance allows the Gaussian quadratures to be efficiently used for numerical simulation and represent $T_{\Delta\lambda}(m)$ in the form of a short exponential series (as a rule, $N \le 7$–10); g_i and C_i are the nodes and coefficients of the Gaussian quadratures; $\sum_{i=1}^{N} C_i = 1$.

To exclude problems associated with the account of overlapped absorption bands of various atmospheric gases, the following calculation technology was applied:

– molecular absorption coefficients were calculated by the line-by-line (LBL) method for a mixture of gases under given meteorological conditions (pressure, temperature, concentration of absorbing gases);

– using these coefficients and the spectral dependence of the solar constant $I_0(\lambda)$ and the instrumental function of the detector $F^*(\lambda)$, the effective absorption coefficients and the coefficients of Gaussian quadratures were calculated by the k-distribution method.

2. Simulation of radiative characteristics: horizontally homogeneous atmosphere

2.1. Model of the atmosphere

The horizontally homogeneous model of the atmosphere was defined as a set of N_{lay} layers with constant pressure, temperature, humidity, etc. Each jth layer, $1 \le j \le N_{\mathrm{lay}}$, was described by a constant aerosol extinction coefficient $\sigma_j^{\mathrm{aer}}(\lambda)$, single scattering albedo $\varpi_j^{\mathrm{aer}}(\lambda)$, and the scattering phase function $g_j^{\mathrm{aer}}(\mu, \lambda)$, where μ is the cosine of the scattering angle. The vertical stratification of the aerosol optical properties corresponded to the model recommended by the World Climate Program (WCP).[9] This model includes the values of $\sigma_j^{\mathrm{aer}}(\lambda)$, $\varpi_j^{\mathrm{aer}}(\lambda)$, and $g_j^{\mathrm{aer}}(\mu, \lambda)$ for fixed (reference) wavelengths; for other λ the values of the optical characteristics are obtained through linear interpolation. The molecular (Rayleigh) scattering coefficient $\sigma_j^{\mathrm{r}}(\lambda)$ was defined within each layer as well.[10]

Clouds were considered as a separate layer (number N_{cl}) with the bottom $H_{\mathrm{b}}^{\mathrm{cl}}$ and top $H_{\mathrm{t}}^{\mathrm{cl}}$ boundaries. The optical model of clouds was determined by the extinction coefficient $\sigma^{\mathrm{cl}}(\lambda)$, single scattering albedo $\varpi^{\mathrm{cl}}(\lambda)$, and the scattering phase function $g^{\mathrm{cl}}(\mu, \lambda)$. These characteristics were calculated for fixed wavelengths based on the Mie theory[11] on the assumption that the size distribution of cloud droplets satisfies a Γ-distribution with the parameters corresponding to the "wide" distribution of particles.[12] To take into account the spectral dependence of the optical characteristics of clouds, linear interpolation was used for the intermediate values of λ.

It was assumed that the underlying surface reflects the incident radiation according to Lambert law with the albedo A_{s}.

2.2. Computational algorithms

For the calculation of the spectral radiative characteristics $R_{\Delta\lambda}$ (flux, brightness) taking into account the molecular absorption, we used two different algorithms based on the solution of the radiative transfer equation by the Monte Carlo method.[13,14]

The first algorithm is based on the possibility (according to Eq. (2)) of representing $R_{\Delta\lambda}$ as a sum

$$R_{\Delta\lambda} = \sum_{i=1}^{N} C_i R_i, \quad (3)$$

where R_i is the monochromatic radiation at the cumulative wavelength g_i, corresponding to the ith set of the effective molecular absorption coefficients

$$\{k^i(z)\}_{i=1}^N, \;\; k^i(z) \equiv k(g_i, z).$$

Within the spectral interval $\Delta\lambda$, the optical characteristics of clouds and aerosol, as well as the Rayleigh scattering coefficients were assumed constant. For all $1 \le i \le N$ in the jth layer, the scattering coefficients of the medium remain unchanged and were determined by the equations:

$$\sigma_{s,j}^{mix,1} = \omega^{cl}\sigma^{cl} + \omega_j^{aer}\sigma_j^{aer} + \sigma_j^r, \;\; j = N_{cl},$$
$$\sigma_{s,j}^{mix,1} = \omega_j^{aer}\sigma_j^{aer} + \sigma_j^r, \;\; j \ne N_{cl}, \tag{4}$$

whereas the extinction coefficient of the medium at the ith step varied as

$$\sigma_j^{mix,1} = \sigma^{cl} + \sigma_j^{aer} + \sigma_j^r + k_j^i, \;\; j = N_{cl},$$
$$\sigma_j^{mix,1} = \sigma_j^{aer} + \sigma_j^r + k_j^i, \;\; j \ne N_{cl}. \tag{5}$$

The absorption by atmospheric gases was taken into account at every photon impact through the quantum survival probability:

$$\omega_j^{mix,1} = \sigma_{s,j}^{mix,1} \big/ \sigma_j^{mix,1}.$$

The second algorithm is based on the Van de Hulst and Irvine's idea[12] that events of absorption and scattering of optical radiation are independent. According to this approach, the selection of the photon trajectory is simulated in the medium with molecular absorption ignored, that is, in contrast to Eq. (5), the extinction coefficient is determined by the equation

$$\sigma_j^{mix,2} = \sigma^{cl} + \sigma_j^{aer} + \sigma_j^r, \;\; j = N_{cl};$$
$$\sigma_j^{mix,2} = \sigma_j^{aer} + \sigma_j^r, \;\; j \ne N_{cl}. \tag{5a}$$

The molecular absorption at every impact point $\mathbf{r}_n$ is taken into account by introducing the additional statistical photon weight, which is determined by the transmission function and decreases with the increase of the distance L [Refs. 13 and 14]:

$$L = \sum_{k=1}^{n} l_k, \;\; l_k = |\mathbf{r}_k - \mathbf{r}_{k-1}|.$$

In both of the algorithms, the photon trajectories were simulated by the standard method.[13]

The first algorithm is more time-consuming as compared with the second one, because to find $R_{\Delta\lambda}$, it is necessary to perform N calculations in media with different values of the extinction coefficient (5). The greater is the number N of terms in the series used for the approximation of the transmission function by the exponential series (2), the longer is the time needed for calculation of one or another radiative characteristic.

2.3. Test calculations

To test these algorithms, we compared our results with the reference calculations of upward and downward going fluxes for the cloudless atmosphere from Ref. 15.

Initially, the errors due to application of the exponential series were estimated. Table 1 gives the values of the transmitted radiation for the 10000–10500 cm^{-1} (950–1000 nm) band in the purely absorbing atmosphere as calculated by the LBL and k-distribution methods for different numbers of terms of series N in Eq. (2).

The LBL calculations were performed using the suite of programs developed in the IAO SB RAS[16]; the high computational speed was provided by the use of the multigrid algorithm. Spectral line parameters were taken from the HITRAN-92 and HITRAN-2000 databases (http://www.hitran.com), and the solar constant was taken from LOWTRAN-7 [Ref. 10]. The HITRAN-92 database and the solar constant from LOWTRAN-7 were used, because the Fomin's calculations[15] were made just for these initial data. The continuum absorption was calculated by the CKD 2.4 model developed by Clough with co-workers (http://rtweb.aer.com). The vertical profiles of temperature, air pressure, and the concentrations of atmospheric gases (H_2O, CO_2, O_3, CH_4, and others) were set according to the AFGL meteorological model for the mid-latitudinal summer.[17]

Our calculations by the LBL method with the use of the HITRAN-92 data coincide with the results from Ref. 15 accurate to 0.1%. The differences in the downward fluxes caused by the transition to HITRAN-2000 in the 10000–10500 cm^{-1} band under consideration increase up to ~2% at the surface layer. The relative error of the values calculated with the aid of the k-distribution method as compared with the LBL method depend on the number of quadratures N: thus, for example, if at $N = 4$ the error did not exceed 1%, then at $N = 10$ it dropped down to ~0.1%. The number of quadratures depends on the spectral range considered and the requirements imposed on the accuracy of the radiative calculations in every particular problem. Since this study involved the comparison of the calculated data with the field measurement data, for approximation of the transmission function in the further calculations we restricted our consideration to the series of four terms: in this case the error in calculated data on the transmittance and fluxes was largely within 1%.

Table 2 gives the values of the upward ($F_{clr}^{\uparrow}$) and downward ($F_{clr}^{\downarrow}$) fluxes of solar radiation calculated by the first and second methods (see Section 2.2) in the molecular–aerosol atmosphere. The calculations were made in the 10000–10500 cm^{-1} band at $N = 4$ for the maritime I aerosol profile[9] and correspond to the 50th and 51st ICRCCM standard sets.[18] The difference between fluxes calculated by the first and second methods does not exceed 0.05–0.1%, which is much smaller than the error due to the use of the short exponential series.

Table 1. Test calculations of downwelling fluxes (W/m^2) in the spectral range of 10000–10500 cm^{-1} in the purely absorbing atmosphere performed with the aid of the HITRAN-92 and HITRAN-2000 databases; solar constant is borrowed from Ref. 10; meteorological model – mid-latitudinal summer (MLS)[17]; solar zenith angle $\xi_{\odot}=30°$; $\Delta = F_{\Delta\lambda}^{\downarrow,\mathrm{LBL}} - F_{\Delta\lambda}^{\downarrow,k(N)}$ is the difference between the LBL calculation and the calculation by the *k*-distribution method with different number of quadratures *N*

z, km	HITRAN-92						HITRAN-2000		
	Ref. 15	Our calculations							
	LBL	LBL	*k*-distr., N = 4	Δ	*k*-distr., N = 10	Δ	LBL	*k*-distr., N = 4	Δ
100.0	31.448	31.449	31.451	–0.002	31.451	–0.002	31.449	31.451	–0.002
70.0	31.448	31.449	31.451	–0.002	31.451	–0.002	31.449	31.451	–0.002
50.0	31.448	31.449	31.451	–0.002	31.451	–0.002	31.449	31.451	–0.002
20.0	31.446	31.446	31.449	–0.003	31.449	–0.003	31.446	31.449	–0.003
15.0	31.443	31.444	31.448	–0.004	31.447	–0.003	31.444	31.448	–0.004
14.0	31.442	31.443	31.448	–0.005	31.447	–0.004	31.443	31.448	–0.005
13.0	31.441	31.442	31.447	–0.005	31.446	–0.004	31.442	31.447	–0.005
12.0	31.437	31.439	31.446	–0.007	31.443	–0.004	31.438	31.446	–0.008
11.0	31.424	31.425	31.442	–0.017	31.433	–0.008	31.424	31.441	–0.017
10.0	31.383	31.385	31.426	–0.041	31.400	–0.015	31.381	31.424	–0.043
9.0	31.303	31.304	31.389	–0.085	31.329	–0.025	31.295	31.385	–0.090
8.0	31.170	31.170	31.317	–0.147	31.202	–0.032	31.153	31.308	–0.155
7.0	30.956	30.956	31.181	–0.225	30.988	–0.032	30.927	31.163	–0.236
6.0	30.637	30.637	30.937	–0.300	30.655	–0.018	30.592	30.904	–0.312
5.0	30.183	30.182	30.523	–0.341	30.177	0.005	30.114	30.466	–0.352
4.0	29.492	29.489	29.788	–0.299	29.467	0.022	29.389	29.692	–0.303
3.0	28.456	28.477	28.597	–0.12	28.466	0.011	28.329	28.440	–0.111
2.0	27.039	27.066	26.911	0.155	27.074	–0.008	26.853	26.680	0.173
1.0	25.278	25.295	25.002	0.293	25.305	–0.010	25.001	24.709	0.292
0.0	23.260	23.274	23.132	0.142	23.298	–0.024	22.890	22.779	0.111

Table 2. Upward and downward going radiation fluxes $F_{\mathrm{clr}}^{\uparrow}(z)/F_{\mathrm{clr}}^{\downarrow}(z)$ (W/m^2) in the gas–aerosol atmosphere in the 10000–10500 cm^{-1} spectral range, calculated by two different methods (Section 2.2); the number of terms in the series N = 4; MLS meteorological model[17]; maritime I aerosol model[9]; solar zenith angle $\xi_{\odot}$ = 30°

z, km	A_s = 0					A_s = 0.8				
	Ref. 15	Our calculations				Ref. 15	Our calculations			
	LBL	Method 1	Method 2	Method 1	Method 2	LBL	Method 1	Method 2	Method 1	Method 2
	HITRAN-92			HITRAN-2000		HITRAN-92			HITRAN-2000	
0	0 / 22.87	0 / 22.74	0 / 22.74	0 / 22.40	0 / 22.39	18.57 / 23.22	18.48 / 23.10	18.48 / 23.10	18.20 / 22.74	18.20 / 22.73
1	0.0592 / 24.96	0.061 / 24.68	0.0616 / 24.68	0.0599 / 24.40	0.0603 / 24.39	16.84 / 25.21	16.90 / 24.94	16.90 / 24.94	16.55 / 24.64	16.54 / 24.64
2	0.117 / 26.79	0.121 / 26.66	0.121 / 26.67	0.118 / 26.43	0.118 / 26.45	16.08 / 26.94	16.18 / 26.82	16.17 / 26.83	15.79 / 26.59	15.78 / 26.60
3	0.128 / 28.23	0.132 / 28.36	0.132 / 28.35	0.129 / 28.21	0.130 / 28.23	15.74 / 28.36	15.84 / 28.51	15.84 / 28.50	15.44 / 28.35	15.43 / 28.37
4	0.142 / 29.28	0.146 / 29.57	0.146 / 29.56	0.142 / 29.48	0.143 / 29.47	15.57 / 29.41	15.68 / 29.71	15.68 / 29.69	15.27 / 29.61	15.27 / 29.60
5	0.154 / 30.00	0.16 / 30.33	0.16 / 30.34	0.157 / 30.28	0.157 / 30.26	15.48 / 30.11	15.60 / 30.45	15.59 / 30.45	15.18 / 30.39	15.18 / 30.37
10	0.219 / 31.31	0.224 / 31.35	0.224 / 31.34	0.221 / 31.35	0.221 / 31.34	15.38 / 31.36	15.49 / 31.40	15.49 / 31.39	15.07 / 31.40	15.07 / 31.39
12	0.239 / 31.40	0.245 / 31.41	0.245 / 31.38	0.242 / 31.41	0.232 / 31.43	15.36 / 31.43	15.47 / 31.44	15.47 / 31.42	15.06 / 31.44	15.06 / 31.46
20	0.264 / 31.44	0.274 / 31.44	0.274 / 31.46	0.27 / 31.44	0.27 / 31.46	15.37 / 31.44	15.48 / 31.45	15.48 / 31.47	15.06 / 31.45	15.06 / 31.47
50	0.274 / 31.45	0.286 / 31.45	0.286 / 31.47	0.282 / 31.45	0.283 / 31.47	15.37 / 31.45	15.48 / 31.45	15.48 / 31.47	15.07 / 31.45	15.06 / 31.47
70	0.274 / 31.45	0.286 / 31.45	0.286 / 31.47	0.283 / 31.45	0.283 / 31.47	15.37 / 31.45	15.48 / 31.45	15.48 / 31.47	15.07 / 31.45	15.06 / 31.47
100	0.274 / 31.45	0.286 / 31.45	0.286 / 31.45	0.283 / 31.45	0.283 / 31.45	15.37 / 31.45	15.48 / 31.45	15.48 / 31.45	15.07 / 31.45	15.06 / 31.45

The calculated reference results,[15] presented in Table 2, were obtained by the LBL method. The analysis of these results shows that if using the HITRAN-92, the representation of the transmission function as a sum of four exponents leads to overestimation of the downwelling fluxes at the altitudes $z \geq 3$ km and their underestimation near the surface ($z \leq 2$ km) as compared with the estimates by LBL method. Analogous pattern can be seen in Table 1 as well. Rather significant (> 0.15 W/m^2) differences in $F^{\downarrow}_{\text{clr}}$ at the altitude $z \leq 3$ km (see the 3rd, 5th and 4th, 6th columns in Table 2) are caused by the transition from HITRAN-92 to HITRAN-2000 (for comparison see Table 1).

3. Comparison of model calculations and experimental data

In this Section, the simulated spectral fluxes of solar radiation are compared with observations obtained for cases of single-layer low-level continuous cloudiness during the ARM (Atmospheric Radiation Measurement) campaign of 1997–1998 at the SGP (Southern Great Plains) site (Oklahoma, USA).[19,20]

3.1. Data of field experiments

The data on the spectral fluxes were obtained with the Rotating Shadowband Spectroradiometer (RSS), which measures the direct, diffuse, and net radiation in 512/1024 channels within the optical region (350–1075 nm) (see, for example, Ref. 21). The vertical profiles of the pressure, temperature, and water vapor were retrieved from radiosonde data, while the liquid water path (LWP) of clouds was retrieved from the data of microwave sensing. The information about total ozone content was taken from the TOMS (Total Ozone Mapping Spectrometer) archive. The top and bottom boundaries of the cloud layer were determined with the aid of ground-based radars. The calculations accounted for the spectral behavior of the surface albedo derived from the MFRSR (Multi-filter Rotating Shadowband Radiometer) measurements.[22] The cloud extinction coefficient was chosen so that the calculated and measured spectral fluxes coincided in the 500–550 nm band. The effective radius of cloud droplets r_{eff}, determined as

$$r_{\text{eff}} = \frac{3\text{LWP}}{2\sigma^{\text{cl}}(H_{\text{t}}^{\text{cl}} - H_{\text{b}}^{\text{cl}})\rho}$$

(ρ is the water density), varied in the range from 6 to 11 μm and corresponded to the typical values of stratus clouds in the region under study.[23]

3.2. Influence of filter function on the calculated results

In the spectral ranges, where the molecular absorption is weak, the transmission function is often calculated with the use of the approximate description of the spectral dependence of the instrumental function $F^*(\lambda)$ in the rectangular form. However, in the presence of molecular absorption, this approximation can lead to marked errors in radiative calculations.[24]

It is assumed that the reference model RSS profile, closest to the real one, in the bands centered at λ_0 is well approximated by the truncated Gaussian function (ftp://oink.asrc.cestm.albany.edu/pub/RSS102):

$$F(\lambda,\lambda_0) = \exp\left(-\left((\lambda-\lambda_0)/w(\lambda_0)\right)^2\right)$$
$$\text{at } |\lambda-\lambda_0| \leq \lambda_{0,\max},$$

where $\lambda_{0,\max}$ was determined from the condition

$$F(\lambda_{0,\max},\lambda_0) = 0.02;$$
$$\text{for } |\lambda-\lambda_0| > \lambda_{0,\max}\ F(\lambda_0,\lambda) = 0.$$

Estimate the error in the transmission function $T_{\Delta\lambda}(m)$, which arises as the reference profile is replaced with its approximation in the rectangular shape (spectral width of the rectangular instrumental function was equal to the spectral width of the Gaussian instrumental function at the exp(–1) level):

$$\delta_T = 100\%\left(T_{\Delta\lambda}^{\text{rect}}(m) - T_{\Delta\lambda}^{\text{Gaus}}(m)\right)/T_{\Delta\lambda}^{\text{Gaus}}(m).$$

The effective absorption coefficients were calculated using the HITRAN-2000 database; the values of the extraterrestrial solar constant were taken from Refs. 25 and 26. The number of terms of the series in the representation (2) was taken $N = 4$. Figure 1 depicts the spectral fluxes of the solar radiation at the top boundary of the atmosphere ($z = H_{\text{atm}} = 100$ km and at the surface level $z = 0$), calculated by the LBL method for the case of purely absorbing atmosphere.

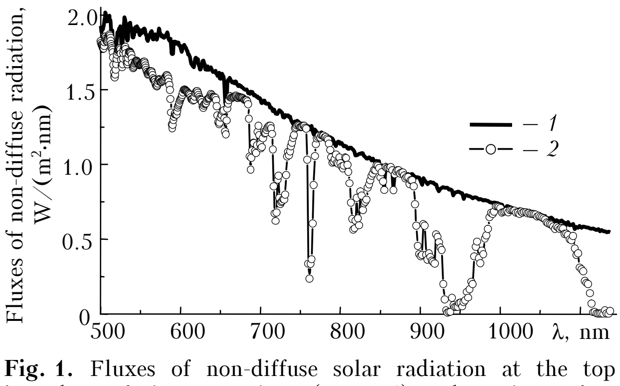

Fig. 1. Fluxes of non-diffuse solar radiation at the top boundary of the atmosphere (curve *1*) and at the surface level (curve *2*), calculated by the LBL method for the case of purely absorbing atmosphere. Curves shown in Figs. 1–4 were obtained using the HITRAN-2000 database; the solar constant was taken from Ref. 26; the meteorological model is mid-latitudinal summer[17]; $\xi_{\odot}$=75°.

The calculations showed that δ_T increases with the increasing absorption of the solar radiation by atmospheric gases, and at the solar zenith angle $\xi_{\odot} = 75°$ it is $\approx 2\%$ at $\lambda = 591$ nm and $\approx 8\%$ at $\lambda = 761$ nm. In the 940 nm water vapor absorption band, the values of δ_T achieve $\approx 25\%$, and at $\lambda = 947$ nm $\delta_T \approx 330\%$ (Fig. 2). This means that to improve the accuracy of radiative calculations, it is needed to take into account instrumental functions of real devices even in the bands of relatively weak absorption by atmospheric gases.

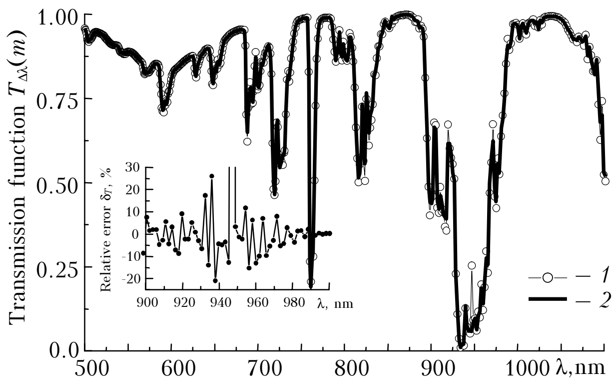

Fig. 2. Transmittance in the purely absorbing atmosphere (LBL method): instrumental function in the form of the truncated Gaussian function (curve *1*) and rectangular instrumental function (curve *2*). The relative error δ_T (%) of the transmission function when using the rectangular function in place of the truncated Gaussian function in shown in the inset; $\xi_{\odot}$=75°.

3.3. Comparison of model calculations with experimental data

We have calculated the spectral fluxes in the 550–650 nm band for three different cloud situations (Table 3) using the second algorithm (see Section 2.2). The effective molecular absorption coefficients were calculated taking into account the filter function of the RSS radiometer (512 channels). The aerosol characteristics corresponded to the cont-I model of the continental aerosol.[9] Scattering in clouds was simulated using the Heney–Greenstein scattering phase function with the mean cosine $\langle\mu\rangle = 0.86$.

The comparison with the experiment showed that in all the cases considered our calculations are in a satisfactory agreement with both the experimental data and the calculations made in Ref. 19 with the use of the MODTRAN4 code. In some cases, our results were in a better agreement with the measured spectral fluxes than the MODTRAN4 calculations (Fig. 3). Thus, the algorithms proposed by us are generally adequate to the process of solar radiation transfer in the horizontally homogeneous atmosphere.

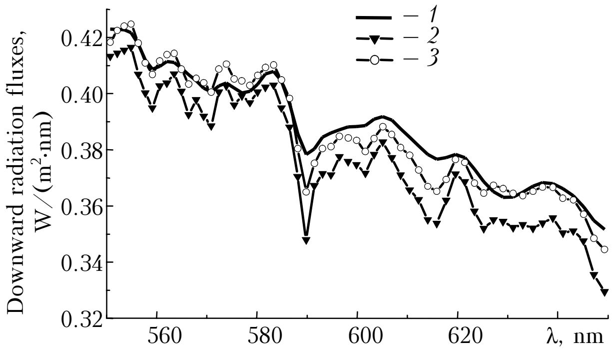

Fig. 3. Downward going sunlight fluxes at the surface level for the cloud situation of October 19 of 1997 (Table 3): RSS (512 channels) measurements (curve *1*); model calculations,[19] rural aerosol, visibility range of 23 km (curve *2*); our calculations, cont-I aerosol profile[9] (curve *3*).

4. Simulation of the radiative characteristics: broken clouds

The optical model of broken clouds was defined within the layer $H_b^{cl} \le z \le H_t^{cl}$ in the form of random scalar fields of the extinction coefficient $\sigma^{cl}(\lambda)\kappa(\mathbf{r})$, single scattering albedo $w^{cl}(\lambda)\kappa(\mathbf{r})$, and scattering phase function $g^{cl}(\lambda, \mu)\kappa(\mathbf{r})$. The mathematical model of the statistically homogeneous field $\kappa(\mathbf{r})$ is constructed based on Poisson dot flows on straight lines and its description can be found, for example, in Ref. 27.

The algorithm for calculation of average (over cloud realizations) radiative characteristics in broken clouds is described in Ref. 5. The algorithms, essentially, involve, first, the separation of the range into N_{int} subranges, assuming that within each of them the optical characteristics of clouds and aerosol are constant and, second, the calculation of spectral fluxes by the Monte Carlo method developed for solution of the system of closed equations for the mean intensity.[5,27] To take the molecular absorption into account, it is proposed to use one or another parameterization of the transmission function (this approach corresponds to the second algorithm described in Section 2.2 for the horizontally homogeneous atmosphere).

Table 3. Atmospheric parameters used as input data in calculations of spectral sunlight fluxes; experiments were conducted as Atmospheric Radiation Measurement Southern Great Plains site (USA)

Date	Solar zenith angle, deg.	Total content, cm			Position of the cloud layer, km	Cloud optical depth at 550 nm	Effective radius, μm
		water vapor	liquid water	ozone			
Oct 19 1997	47.15	1.6	0.008	0.34	0.58–0.85	16.5	7.2
Apr 03 1998	31.17	1.4	0.034	0.38	1.0–1.5	55.1	9.3
Aug 05 1998	24.39	4.1	0.019	0.33	1.49–1.88	25.9	9.1

In contrast to Ref. 5, where the results of Refs. 6 and 7 were used for approximation of the transmission function $T_{\Delta\lambda}$, in this paper $T_{\Delta\lambda}$ is represented in the form of the exponential series. The effective molecular absorption coefficients are calculated based on the HITRAN-2000 database for any real profiles of temperature, pressure, and concentrations of atmospheric gases taking into account the instrumental function of real devices.

Figure 4 shows an example of the average spectral fluxes of the upwelling $\langle F^{\uparrow}\rangle$ and downwelling $\langle F^{\downarrow}\rangle$ solar radiation in broken clouds calculated using the modification mentioned above.

The effective molecular absorption coefficients were calculated using the instrumental functions of the RSS radiometer (1024 channels). Figure 4 also shows the results of simulation of $\hat{F}^{\uparrow(\downarrow)}$ on the assumption of horizontally homogeneous clouds:

$$\hat{F}^{\uparrow(\downarrow)} = pF_{\rm pp}^{\uparrow(\downarrow)} + (1-p)F_{\rm clr}^{\uparrow(\downarrow)}, \qquad (6)$$

where p is the cloud amount index, and the subscripts pp and clr correspond to the fluxes under the overcast conditions and for clear sky. The results shown in Fig. 4 are in a good agreement with our earlier conclusions about the influence of the random cloud geometry on the transfer of optical radiation in the atmosphere.[27]

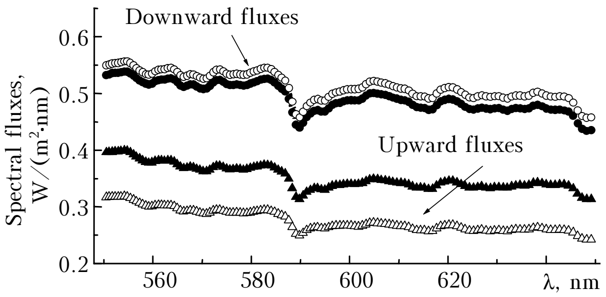

Fig. 4. Average fluxes of diffuse radiation at the surface level $\langle F^{\downarrow}(z=0)\rangle$ and at the top boundary of the atmosphere $\langle F^{\uparrow}(z = H_{\rm atm})\rangle$ (closed signs); cloud amount index $p = 0.5$; mean cloud size $D = 0.5$ km; cloud layer of 1–2 km; $\xi_{\odot} = 60°$, $\sigma(\lambda = 550\ \text{nm}) = 10\ \text{km}^{-1}$; $A_s = 0.2$; open signs correspond to the calculation in the horizontally homogeneous atmosphere (6).

Note that at the high spectral resolution the number $N_{\rm int}$ can be large enough. To decrease the time needed for calculation of spectral fluxes (brightness) both in the horizontally homogeneous atmosphere and in broken clouds, the algorithm based on the dependent test method[5,13] can be used. This approach is not discussed here, but whenever necessary, it will be implemented taking into account the modifications proposed in this study.

Conclusions

In this paper, we have presented the algorithms for calculation of spectral fluxes (brightness) of the solar radiation in the atmosphere taking into account the absorption by atmospheric gases. The spectral range of interest is divided into $N_{\rm int}$ smaller subranges in accordance with the needed spectral resolution in such a way that within each of the subranges the spectral variability of aerosol and cloud optical characteristics can be neglected. The radiative characteristics are calculated by the Monte Carlo method; the molecular absorption is taken into account through the quantum survival probability or through the additional photon weight, determined by the transmission function and decreasing with the increase of the distance traveled by the photon. The transmission function is approximated by the exponential series (k-distribution method). The effective molecular absorption coefficients are calculated based on the HITRAN-2000 spectroscopic database with the allowance for real profiles of meteorological parameters and concentrations of atmospheric gases, as well as the instrumental functions of real devices. The number of terms in the series depends on the spectral range considered and on the requirements imposed on the accuracy of radiative calculations.

The comparative analysis has demonstrated good agreement between the results obtained and the data of reference LBL calculations preformed by other authors. The agreement between our calculated data and data of the Rotating Shadowband Spectroradiometer measurements at the ARM SGP site (USA) for the spectral fluxes under conditions of continuous, horizontally homogeneous low-level clouds confirms that the algorithms proposed are adequate to the process of the solar radiation transfer in the atmosphere.

In addition, this paper has described a modification of the algorithm developed earlier[5] for the calculation of the average spectral radiative characteristics in broken clouds. In addition to the effect of the random cloud geometry, this model also accounts for the latest achievements of atmospheric spectroscopy. This permits a more adequate simulation of regularities of the solar radiation transformation in the atmosphere.

Acknowledgments

The experimental data on spectral fluxes and atmospheric parameters from the ARM SGP site (USA), as well as the calculations based on the radiative transfer code MODTRAN4, were kindly placed at our disposal by A.P. Trishchenko (Canada Centre for Remote Sensing, Ottawa, Canada) and M. Cribb (at that time, Intermap Technologies Ltd, Ottawa, Canada). We are also grateful to Lee Harrison and Peter Kiedron (Atmospheric Sciences Research Center, State University of New York, Albany, USA) for the information about the characteristics of Rotating Shadowband Spectroradiometer, needed for this investigation.

This work was supported, in part, by the DOE's ARM Program (contract No. 5012) and the Russian

Foundation for Basic Research (grants No. 03-05-64655 and No. 04-07-90123).

References

1. S.A. Clough, M.J. Iacono, and J.L. Moncet, J. Geophys. Res. D **97**, 16519–16535 (1992).
2. J.L. Moncet and S.A. Clough, J. Geophys. Res. D **102**, No. 18, 21853–21866 (1997).
3. W. O'Hirok and C. Gautier, J. Atmos. Sci. **55**, 2162–2179 (1998).
4. W. O'Hirok and C. Gautier, in: *Proc. of the Tenth Atmospheric Radiation Measurement (ARM) Science Team Meeting*, available URL: http://www.arm.gov/docs/documents/technical/conf_0003/ohirok-00.pdf.
5. G.A. Titov, T.B. Zhuravleva, and V.E. Zuev, J. Geophys. Res. D **102**, No. 2, 1819–1832 (1997).
6. B.M. Golubitskii and N.I. Moskalenko, Izv. Akad. Nauk SSSR, Fiz. Atmos. Okeana **IV**, No. 3, 346–360 (1968).
7. N.I. Moskalenko, Izv. Akad. Nauk SSSR, Fiz. Atmos. Okeana **V**, No. 11, 1180–1190 (1969).
8. K.M. Firsov, T.Yu. Chesnokova, V.V. Belov, A.B. Serebrennikov, and Yu.N. Ponomarev, Vychisl. Tekhnol. **7**, No. 5, 77–87 (2002).
9. *A Preliminary Cloudless Standard Atmosphere for Radiation Computation. World Climate Research Programme*, WCP-112, WMO/TD No. 24 (1986), 60 pp.
10. F.X. Kneizys, D.S. Robertson, L.W. Abreu, P. Acharya, G.P. Anderson, L.S. Rothman, J.H. Chetwynd, J.E.A. Selby, E.P. Shetle, W.O. Gallery, A. Berk, S.A. Clough, and L.S. Bernstein, *The MODTRAN 2/3 report and LOWTRAN 7 Model* (Phillips Laboratory, Geophysics Directorate, Hanscom AFB, MA 01731–3010, 1996), 260 pp.
11. D. Deirmendjian, *Electromagnetic Scattering on Spherical Polydispersions* (American Elsevier, New York, 1969).
12. *Radiation in the Cloudy Atmosphere* (Gidrometeoizdat, Leningrad, 1981), 280 pp.
13. G.I. Marchuk, G.A. Mikhailov, M.A. Nazaraliev, R.A. Darbinyan, B.A. Kargin, and B.S. Elepov, *Monte Carlo Method in Atmospheric Optics* (Nauka, Novosibirsk, 1976), 280 pp.
14. B.A. Kargin, *Statistical Modeling of the Solar Radiation Field in the Atmosphere* (Computer Center SB AS USSR, Novosibirsk, 1984), 206 pp.
15. B.A. Fomin and Yu.V. Gershanov, "*Tables of the benchmark calculations of atmospheric fluxes for ICRCCM test cases. Part II: Shortwave results*," Preprint IAE 5990/1 (Moscow, 1996).
16. A.A. Mitsel, I.V. Ptashnik, K.M. Firsov, and B.A. Fomin, Atmos. Oceanic Opt. **8**, No. 10, 847–850 (1995).
17. G. Anderson, S. Clough, F. Kneizys, J. Chetwynd, and E. Shettle, *AFGL Atmospheric Constituent Profiles* (0–120 km) (Air Force Geophysics Laboratory, 1986), AFGL-TR-86-0110. Environm. Res. Paper No. 954.
18. Y. Fouquart and B. Bonnel, J. Geophys. Res. D **96**, No. 5, 8955–8968 (1991).
19. Z. Li, A. Trishchenko, and M. Cribb, in: *Proc. of the Tenth Atmospheric Radiation Measurement (ARM) Science Team Meeting*, available URL: http://www.arm.gov/publications/proceedings/conf10/abstracts/li-z.pdf.
20. Z. Li, M. Cribb, and A. Trishchenko, in: *Proc. of the Eleventh Atmospheric Radiation Measurement (ARM) Science Team Meeting*, available URL: http://www.arm.gov/publictions/proceedings/conf11/abstracts/li-z.pdf.
21. L. Harrison, J. Berndt, P. Kiedron, J. Michalsky, Q. Min and J. Schlemmer, in: *Proc. of the Ninth Atmospheric Radiation Measurement (ARM) Science Team Meeting*, available URL: http://www.arm.gov/docs/documents/technical/conf_9903/harrison-99.pdf.
22. L. Harrison and J. Michalsky, Appl. Opt. **33**, No. 22, 5118–5125 (1994).
23. X. Dong, J. Geophys. Res. D **105**, 4529–4537 (2000).
24. T.B. Zhuravleva, I.M. Nasretdinov, S.M. Sakerin, K.M. Firsov, and T.Yu. Chesnokova, Atmos. Oceanic Opt. **16**, No. 12, 972–981 (2003).
25. J. Fontenla, O.R. White, P.A. Fox, E.H. Avertt, and R.L. Kurucz, Astrophys. J., No. 518, 480–500 (1999).
26. T.L. Kurucz, in: *IAU Symp. 154*, ed. by D.M. Rabin and J.T. Jefferies (Kluwer, Acad. Norwell Massachusetts, 1992).
27. V.E. Zuev and G.A. Titov, *Atmospheric Optics and Climate* (Spektr, Tomsk, 1996), 271 pp.